Highly efficient supramolecular AIE-active pseudorotaxane luminogen for functional bioimaging

Sing Shy Liow,[†] *Hui Zhou,*[†] *Sigit Sugiarto,*[†] *Guo Shifeng,*[†] *Madhavi Latha Somaraju Chalasani,*[‡] *Navin Kumar Verma,*[‡,∥] *Jianwei Xu,*[†] *Xian Jun Loh*[*,†,∥,⊥]

[†]Institute of Materials Research and Engineering (IMRE), 2 Fusionopolis Way, #08-03 Innovis, Singapore 138634, Singapore.

[‡]Lee Kong Chian School of Medicine, Nanyang Technological University, Experimental Medicine Building, Singapore 636921, Singapore.

[∥]Singapore Eye Research Institute, 11 Third Hospital Avenue, The Academia, 20 College Road, Singapore 168751, Singapore.

[⊥]Department of Materials Science and Engineering, National University of Singapore, 9 Engineering Drive 1, Singapore 117576, Singapore.

Corresponding Author

*Xian Jun Loh E-mail: lohxj@imre.a-star.edu.sg

Keywords: AIE micelles, pseudorotaxanes, fluorescence dyes, imaging, tetraphenylethene (TPE)

ABSTRACT: The direct tracking of cells using fluorescent dyes is a constant challenge in cell therapy due to aggregation-induced quenching (ACQ) effect and biocompatibility issues. Here, we demonstrate the development of a biocompatible and highly efficient AIE-active pseudorotaxane luminogen based on tetraphenylethene conjugated poly(ethylene glycol) (TPE-PEG_2) (guest) and α-cyclodextrin (α-CD) (host). It is capable of showing significant fluorescent emission enhancement at 400-600 nm range when excited at 380-388 nm, without increasing the concentration of AIE compound. The fluorescent intensity of TPE-PEG_2 solution was effectively enhanced by 4-12 times with gradual addition of 1-4 mM of α-CD. 2D NOSEY ^{1}H NMR revealed clear correlation spots between the characteristic peaks of α-CD and PEG, indicating the interaction between protons of ethylene glycol and cyclodextrin, and the structures are mainly based on threaded α-CD. The host-guest complex exhibits boosted fluorescent emission because the PEG side chains are confined in "nano-cavities" (host), thus, applying additional restriction on intermolecular rotation of TPE segments. *In vitro* cells experiments demonstrated the potential of AIE-active pseudorotaxane polymer as a biocompatible bioimaging probes.

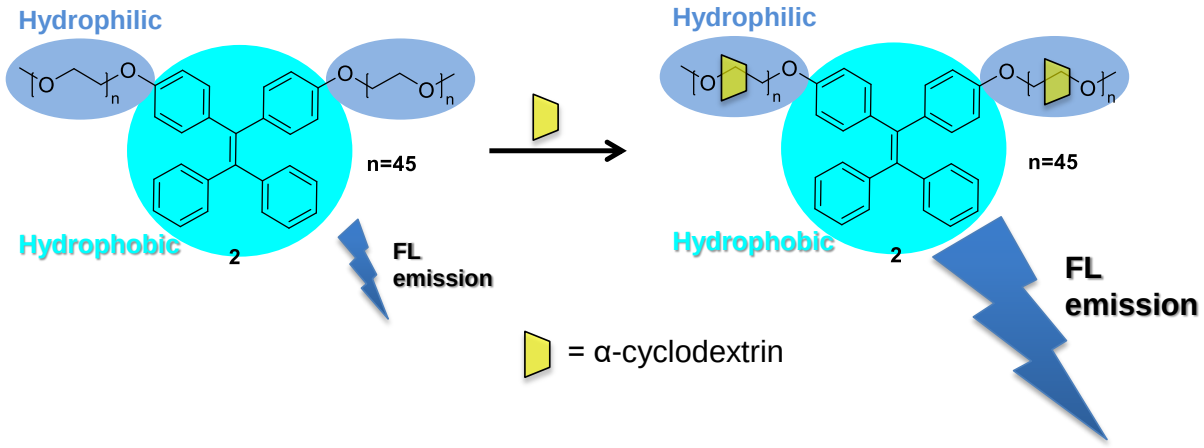

Introduction

Cell-based cancer therapy has shown great promise in recent trials.[1] The major advancement in the cancer treatment is based on T-cell immune therapy, which involves re-engineering of patient's T-cells from blood to attack cancerous cells.[2, 3] The ability to non-invasively track the delivery and function of re-engineered immune cells and the distribution of cancer cells may reveal important information of treatment progress and tumour metastasis.

The direct tracking of cells using fluorescent dyes is a constant challenge in cell therapy due to aggregation-caused quenching (ACQ) effect and biocompatibility issues. Fluorescent dye in the labelled cells exhibits short life-time as a result of ACQ effect, and may leak from cells due to concentration gradient.[4, 5] The fluorescent emission of these molecules is normally quenched when they become aggregated in a complex system like human body due to their poor miscibility in water. Aggregation-induced emission (AIE) fluorescent probes are extensively described[6-10], as perfect luminogens for bioimaging[4, 5, 11], chemical sensors[12, 13] and monitoring of drug delivery[14-16]. AIE molecules emit strong and long-lasting fluorescent when they are aggregated, which behaves in the opposite manner to conventional fluorescent dyes.[17] These molecules emit strong fluorescence when they are aggregated in poor solvent (water) or in solid state; however, when being dispersed in good solvents, they show weak or no emission.[7, 18] The mechanism of AIE characteristic is related to restricted intermolecular rotations (RIR) in aggregated state that limit the non-radiative energy decay pathways.[19] AIE compounds showed strong enhancement of AIE effect resulting from their limited motions in viscous solution/gel such as thermoresponsive hydrogel,[20] or after absorption onto biopolymers such as DNA,[21] or bonded in the inner surface of hollow mesoporous silica tube-like structure.[22] In these micro-environments, AIE effect can be enhanced without increasing concentration of AIE compound.

Theoretically, AIE host-guest inclusion complex could also limit AIE molecular chain motion. However, in a host-guest inclusion complex based on TPE-oligo-ethylene glycol (n=2-4) and γ-CD, fluorescent emission was quenched as a result of de-aggregation of TPE hydrophobic segments when TPE was covered by γ-CD.

AIE host-guest inclusion complex is proposed to be a potentially efficient cell tracking formation, however, there are not many research reports focusing in this area. To understand the interaction between AIE luminogens (guest) and cyclodextrin (host) and their resulting supramolecular structure, in this study, we introduced PEG chains (2000 $g.mol^{-1}$) at two of the side chains of TPE unit, an amphiphilic molecule TPE-PEG_2 with AIE characteristics. Taking the advantage of the formation of pseudorotaxanes (or inclusion complex) between TPE-PEG_2 (guest) and α-cyclodextrin (α-CD) (host), we hypothesized an enhancement in emission efficiency due to restriction of intramolecular motion of TPE without increasing the concentration of fluorescent probes. Continuous increase in fluorescent emission was observed by gradual addition of α-CD. Undesired luminogen uptake by other cell types *in vivo* could be avoided because only the fluorescence intensity of the cells labelled with TPE-PEG_2 would be selectively enhanced. Pseudorotaxanes are supramolecular structures that form between a host (e.g. cyclodextrin, curcubiturils) and guests (e.g. PEG) in aqueous solution due to hydrophobic interaction of the long hydrocarbon chains (guest) with the inner surface of the host.[23] Among the different types of cyclodextrins, α-CD was chosen in this study due to its relatively good solubility in water (as compared to β-CD) with suitable cavity size (inner diameter and cavity depth of 0.45 and 0.67 nm,[24, 25] respectively) to accommodate single PEG chains. PEG-(α-CD) inclusion complex were reported to self-assemble and aggregate in solution, resulting in crystalline pseudorotaxanes stacks in high yields,[26-29] when PEG with molecular weight higher

than 3200 g.mol^{-1} are used.[30] We report the development of a new AIE pseudorotaxane probe based on TPE-PEG_2 and α-CD, which exhibits advantage such as: 1) good biocompatibility, 2) water-solubility, 3) AIE pseudorotaxane luminogen does not leak out from cells, and 4) high emission efficiency for imaging and cell tracking applications. The interaction between AIE luminogens (guest) and cyclodextrin (host) and their resulting supramolecular structure was studied, with a focus on *in vitro* cell traceability, critical micelle concentration (CMC) measurement, biocompatibility studies and fluorescent emission properties. The threading process was examined by using 2D-NOSEY ^{1}H NMR. We also discuss the mechanism of fluorescent emission enhancement.

Materials and Methods

Polyethylene glycol monomethyl ether mesylate with M_n of 2000 Da was purchased from Sigma-Aldrich. Anhydrous dimethylformamide (DMF) was purchased from Merck. Cyclodextrin was supplied by TCI America. All the reactants were used as received.

Molecular characterization

NMR spectra were measured at room temperature using Bruker AV-400 NMR spectrometers in $CDCl_3$. ^{1}H NMR measurement was also carried out as 2D Nuclear Overhauser Enhancement Spectroscopy (2D ^{1}H NMR-NOSEY), using JEOL 500 MHz NMR spectrometer in D_2O. Gel permeation chromatography (GPC) analysis was carried out with a Waters GPC system equipped with Waters Styragel columns, a Waters-2420 ELS detector, at 40 °C. Two columns (10^3 and 10^5Å) (size: 300 × 7.80 mm) were arranged in series. Tetrahydrofuran (HPLC grade) was used as the eluent at a flow rate of 1.0 mL min^{-1}. Monodispersed poly(methyl methacrylate) (PMMA) standards were used to generate the calibration curve. Fourier transform infrared (FTIR)

spectrum (KBr) was recorded on an Pelkin Elmer Spectrum 2000 Spectrometer. 16 scans were signal-averaged with a resolution of 4 cm^{-1} at room temperature.

Synthesis of TPE-PEG_2 (2)

4,4'-(2,2-diphenylethene-1,1-diyl)diphenol (**1**) was prepared according to reference.[31] A mixture of **1** (36.5 mg, 0.1 mmol), polyethylene glycol monomethyl ether mesylate with *Mn* of 2000 Da (600.0 mg, 0.3 mmol) and K_2CO_3 (69.1 mg, 0.5 mmol) were placed in a Schlenk flask, and was dried under vacuum at 60 ^oC for 2 hours. Then anhydrous DMF (1.0 mL) was introduced under argon atmosphere and purge for another 15 min. The reaction mixture was then heated to 120 ^oC for 2 days with stirring. After cooling down, the reaction mixture was extracted with CH_2Cl_2 and washed with deionized water. The organic phase was isolated and dried over $MgSO_4$, followed by filtration and solvents were then removed under vacuum. The crude product was purified by precipitating its solution in THF (2 mL) by Et_2O (250 mL), and the white powder was collected by filtration as 430.0 mg. Yield: 61%. ^1H NMR ($CDCl_3$): δ 3.64 (br). ^{13}C NMR ($CDCl_3$): δ 71.0. IR (thin film): ν = 3436, 2910, 2878, 1644, 1471, 1457, 1352, 1299, 1251, 1103, 952, 845 and 704 cm^{-1}. M_n ~3822 g mol^{-1}, M_w ~4541 g mol^{-1} and PDI ~1.19 obtained by GPC. Ethylene glycol (EG) repeating unit n= 45, based on M_n from supplier. NMR and FTIR graphs were displayed in Figure S1-S3.

Determination of the Critical Micelle Formation Concentration (CMC)

CMC of polymer **2** aqueous solutions was determined by Dynamic light scattering (DLS), using Malvern Zetasizer Nano ZS, at 25 °C. Stock solution was prepared by dissolving small amount of polymer **2** in DI water, equilibrate overnight at room temperature. Concentrations ranging from 2.6×10^{-3} – 2.6 mM were studied. All data were triplicated and the average values were

plotted. The intersection of the tangents to the two slopes of the graph where the log concentration was plotted versus count rate.

Fluorescent properties

Stock solution was prepared by dissolving small amount of polymer **2** in deionized water, equilibrate overnight at room temperature. Concentrations ranging from 2.6×10^{-3} – 2.6 mM were studied. The fluorescence intensity at wavelength of 400 – 600 nm was measured (excited at 388 nm), using a fluorescent spectrophotometer (Shimadzu RF5301). Slit width of 5 was used for excitation and emission.

Atomic force microscope (AFM)

The Nanowizard III instrument (JPK Instruments AG, Berlin, Germany) equipped with the NanoWizard head and controller was used in the AFM measurement. The morphology of the model surfaces was visualized by tapping mode AFM imaging under ambient conditions using standard silicon probes (k ~ 40 N/m, Tap 300AL-G, Budget sensors). All the images were processed using the JPK data processing software (Version 4.2).

Study of cellular internalization of TPE-PEG_2 by confocal microscopy

Cellular uptake of TPE-PEG_2 in the presence of α-CD was determined in A549 cells by confocal microscopy. Cells cultured on 18-mm coverslips were incubated with 2 mg/ml each of TPE-PEG_2 or TPE-PEG_2 + α-CD for 4 h and fixed using 4% formaldehyde in phosphate-buffered saline (PBS). Untreated cells were used as control. After washing with PBS thrice, cells were fluorescently stained with rhodamine phalloidin (Life Technologies) and DRAQ5 (eBiosciences) to visualize cells and nuclei respectively. Following the staining procedure, cells were washed with PBS and mounted on clear glass slides using Flouromount™ Aqueous mounting medium (Sigma-Aldrich). Cellular internalization of TPE-PEG_2 was visualized by LSM 800 Airyscan

microscope using a Plan-Apochromat 1.4 numerical aperture / 63× oil immersion objective lens (Carl Zeiss Microimaging Inc., NY, USA). Three channel images were obtained as a Z-stack (0.45 μm slice thickness) with 405-, 561- and 640 nm excitation lasers. Figures were processed using Zen lite imaging software (Carl Zeiss) and presented. Cellular uptake of TPE-PEG_2 was quantified with the help of IN Cell Investigator software (GE Healthcare Life Sciences). At least 15 different fields for each sample were considered for quantitative analysis.

High Content Analysis (HCA)

Biocompatibility of TPE-PEG_2 and α-CD was assessed using a comprehensive multimodal platform utilizing three different human cell types - alveolar basal epithelial cell line A549, primary dermal fibroblasts (DF) and liver epithelial cell line HepG2 (American Type Culture Collection, ATCC). Cells were cultured in DMEM (Gibco®) supplemented with 10% fetal bovine serum (Gibco®) and Penicillin-Streptomycin antibiotics (Life Technologies, Singapore). For experimental purposes, cells were seeded in 96-well culture plates (Nunc™) at a density of 2000 cells/well and allowed to grow overnight. Cells were then treated with various concentrations of TPE-PEG_2 or α-CD or both (ranging from 62.5 μg/ml to 2000 μg/ml) for 24 h. After washing, cells were fixed by incubating them for 20 min with 4% formaldehyde in PBS. Adherent cells were then fluorescently stained with rhodamine-phalloidin and Alexa Fluor 488 conjugated anti-α-tubulin (Life Technologies) to visualize cellular morphologies and Hoechst 33258 (Sigma-Aldrich) to visualize nuclei. After washing with PBS, plates were scanned using 20X objective, three detection channels with different excitation filters – DAPI filter (461 nm), FITC filter (509 nm) and Cy3 filter (599 nm) and 10 randomly selected fields/well by an automated High Content Screening (HCS) microscope, IN Cell Analyzer 2200 (GE Healthcare). Cell-based multi-parametric quantitative estimation of the acquired images was performed

automatically with IN Cell Investigator software (version 1.6). All the measured quantitative multi-parametric datasets were normalised using their respective percentage change against the corresponding controls and automatically converted in the form of colorimetric gradient heat-maps using TIBCO Spotfire®. Heat-map graphical illustration is considered as the most suitable schematic representation to report variations of multiple quantified parameters. For better visualization of the datasets under the current analysis, minimum values obtained from various parameters were kept "red" through the mean "black" to the maximum "green".

Cell viability assay

Cell viability was studied using MTS-based assay CellTiter 96® AQ_{ueous} One Solution Cell Proliferation Assay kit according to manufacturer's instructions (Promega Corporation, Madison, WI, USA). After the treatment period similar to that of HCA above, cells were incubated with 20 μl of MTS reagent for 2 h at 37°C. Absorbance was recorded at 490 nm using a microplate reader (BioTek) and graphs were platted after subtraction of background absorbance. Treatment was done in triplicates for each sample.

Statistical analysis

Statistical significance of differences among two experimental groups was analyzed by two-tailed unpaired Student's *t* test.

Results and discussion

Synthesis and characterization of TPE-PEG_2 (2)

Amphiphilic TPE-conjugated PEG (**2**) was synthesized based on the scheme provided in Figure 1(a). TPE-PEG_2 was prepared with PEG molecular weight of M_n 2000 $g.mol^{-1}$ on each of the two arms, in *cis* conformation. The 3D structure of TPE-EG_2 (n=1) was shown in 1(b). The purified polymer exhibited molecular weight of M_n 3800 $g.mol^{-1}$, with narrow dispersity index. Molecular characterization datasets, including FTIR, ^{1}H and ^{13}C NMR spectra are given in Figure S1-S3. The polymer is water-soluble and emits bright blue light, in water and in solid bulk (Figure S4), under UV illumination. Photograph of aqueous solutions of the polymer under UV lamp is displayed in Figure 1(c). Concentrations of AIE molecule **2** aqueous solutions are listed in Table 1.

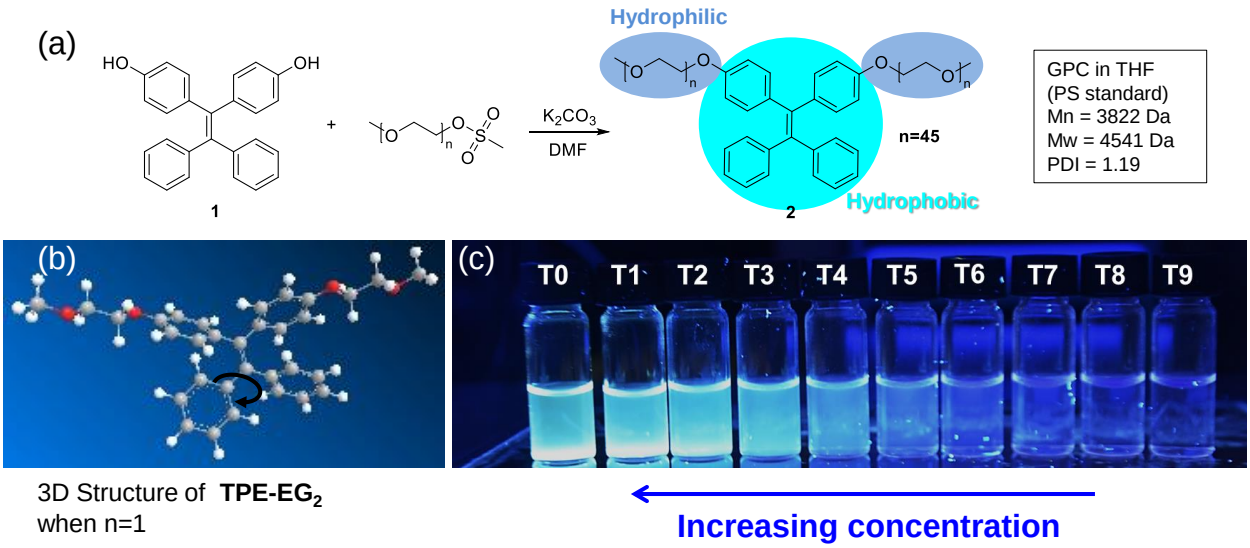

Figure 1. (a) Synthesis procedure of **2**, using 4,4'-(2,2-diphenylethene-1,1-diyl)diphenol (**1**) and polyethylene glycol monomethyl ether mesylate with M_n of 2000 $g.mol^{-1}$. (b) Representative chemical structure of TPE-EG_2 drawn using ChemDraw® 3D, with black arrow indicating RIR. (c) Digital photograph of aqueous solutions of **2** with various concentrations under UV illumination (λ= 365 nm).

Table 1. Sample ID and concentrations of TPE-PEG_2 aqueous solutions

Sample ID	**TPE-PEG_2 conc. (mg/mL)**	**M (mol/L)**
T0	10.0	2.62×10^{-3}

T1	5.0	1.31×10^{-3}
T2	2.5	6.54×10^{-4}
T3	1.25	3.27×10^{-4}
T4	6.25×10^{-1}	1.64×10^{-4}
T5	3.13×10^{-1}	8.18×10^{-5}
T6	1.56×10^{-1}	4.09×10^{-5}
T7	7.81×10^{-2}	2.04×10^{-5}
T8	3.91×10^{-2}	1.02×10^{-5}
T9	1.95×10^{-2}	5.11×10^{-5}
T10	9.77×10^{-3}	2.56×10^{-5}

TPE segments are inherently hydrophobic due to the presence of aromatic rings, [7, 32, 33] while the long PEG chains with M_n of 2000 $g.mol^{-1}$ provide relatively good water-solubility and micelle stability than the amphiphilic molecule in previous study.[34] Critical micelle concentration (CMC) reflects the concentration of the AIE amphiphilic polymer at which micelle starts to form.We performed dynamic light scattering (DLS) analysis to determine the CMC of aqueous solutions of the polymer **2** (Figure 2(a)). In Figure 2 (a), CMC at 25 °C was calculated at 23.7×10^{-5} g/mL (6.2×10^{-5} M) (between T5-T6), where the tangents to the two slopes of the graph intersect. In dilute solution at concentration below CMC, the amphiphilic molecules are in free/unimer state in water. At CMC, they self-assemble and form micelles with the TPE segments aggregated in the core of the micelles. This is a physical association mainly due to hydrophobic interaction and dehydration of PEG segments. As concentration continues to increase, micelles start to form clusters. A schematic drawing of unimers and micelles is shown in Figure 2(b).

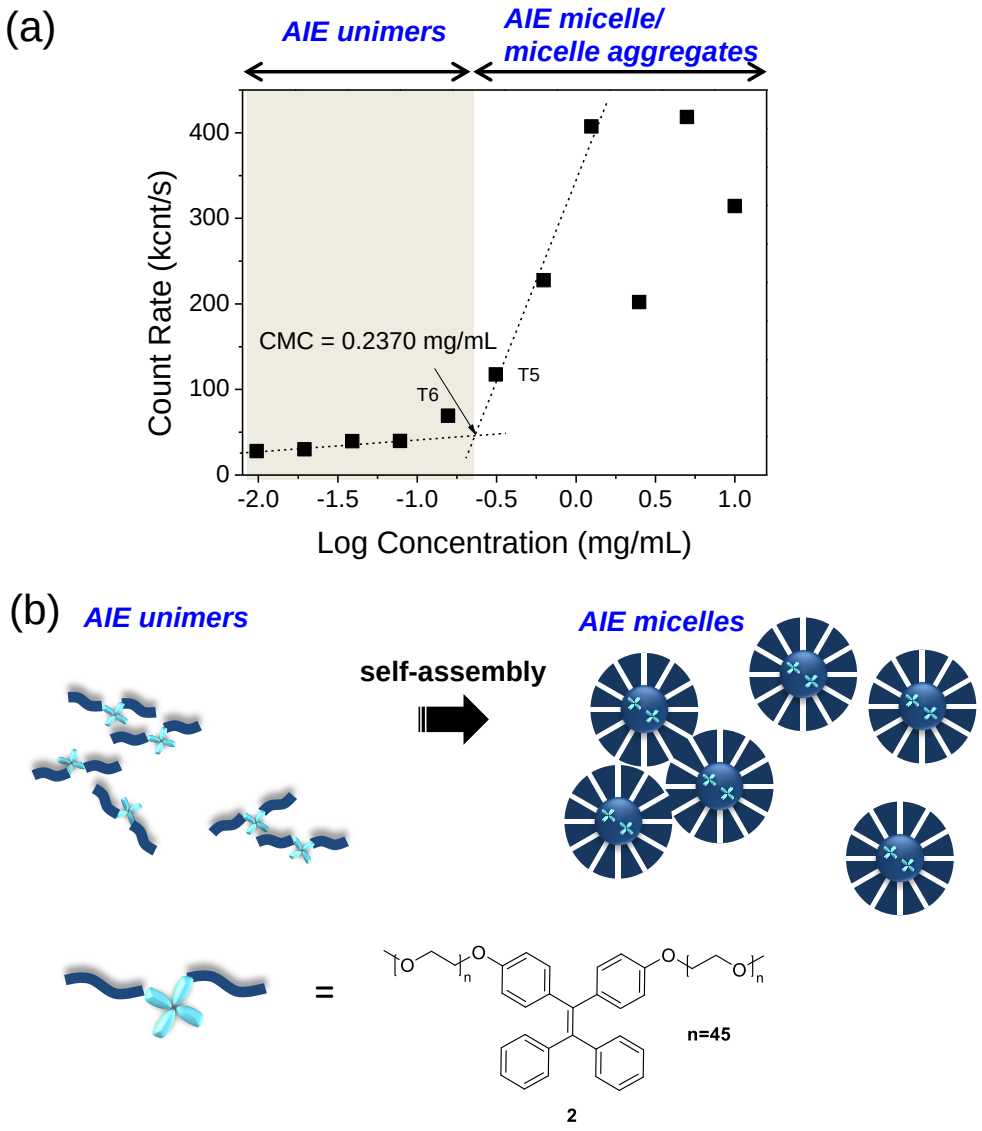

Figure 2. (a) CMC of polymer **2** aqueous solution was in between T5 and T6, determined by DLS at 25 °C. (b) Schematic drawing of self-assembly of AIE micelles.

AIE behavior of aqueous solutions of **2** was characterized by fluorescence assay, as shown in Figure 3. In Figure 3 (a), using excitation wavelength of 388 nm, fluorescent intensity of their polymer solutions increased as the concentration increased at 25 °C. At concentration below CMC (T6 - T10), unimer peak at 448 nm was observed. At T5 (above CMC), broad peak in addition to unimer peak started to appear. As the concentration increased, the AIE solutions

(T0 – T4) exhibited high fluorescent (FL) emission, broadened and red-shifted peak at 464-474 nm, reflecting a more inhomogeneous environment,[35] which could be due to the presence of a mixture of unimers, micelles and micelle aggregates. The enhancement of AIE emission was observed starting from T5 where micelles started to form. The increase in fluorescent intensity due to the formation of micelles (compare unimers state (T10) to micelle state (T5)), was about 2.5 times (250 %). It was attributed to two physical phenomena: i) Intramolecular rotation of TPE was physically restricted by PEG extension. The restricted intramolecular rotation (RIR) blocks non-radiative pathways and leads to fluorescence emission; ii) Further increase in the concentration of polymer resulted in boosted emission due to micelles formation and aggregation of micelles, in which higher degree of rotational restriction was imposed by the surrounding micelles aggregates. Figure 3(b) displayed the fluorescent excitation spectrum of TPE-PEG_2, showing high FL intensity at the range of 370 – 430 nm. AIE behaviour was also characterized FL intensity change in different ratio water/THF (vol %) mixture, as shown in Figure 3(c). The change in intensity was plotted in Figure 3 (d).

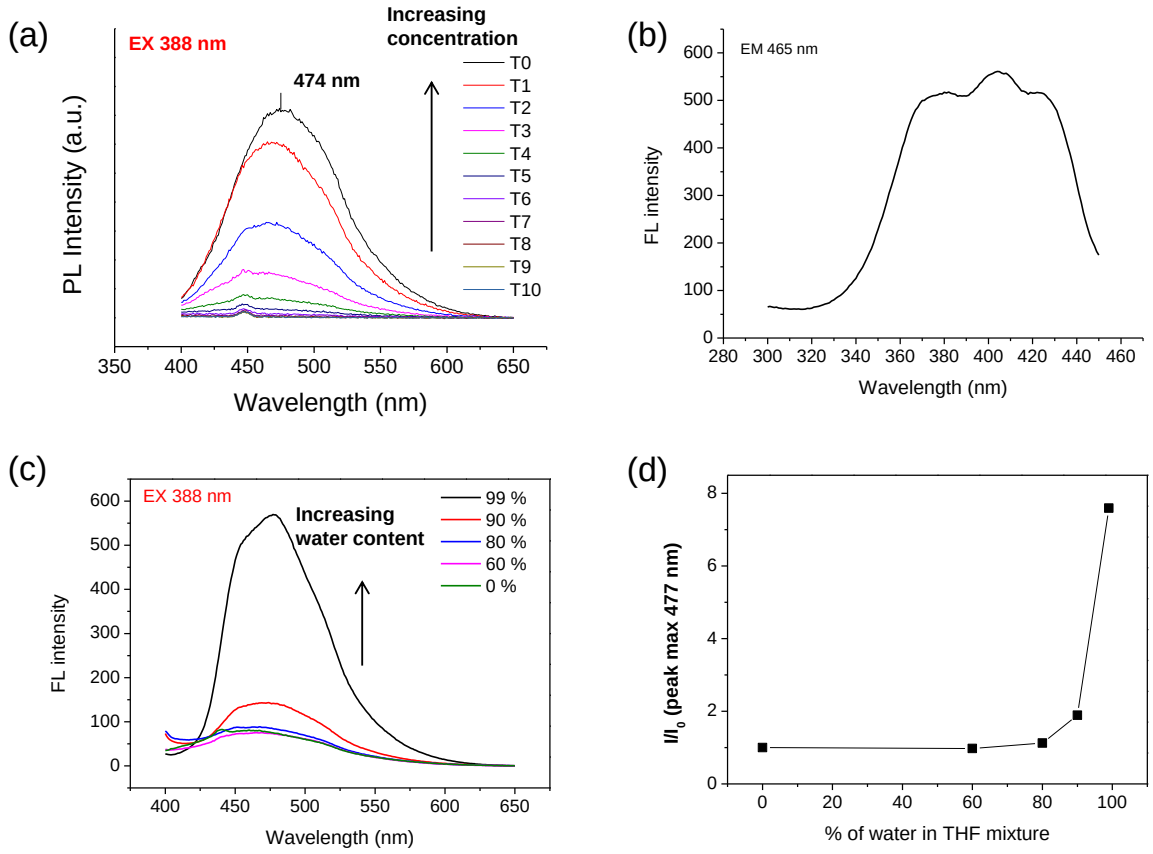

Figure 3. TPE-PEG_2 aqueous solution exhibits AIE behaviour. (a) Fluorescence emission spectra of aqueous solutions of **2** with various concentrations (2.6×10^{-3} – 2.6 mM) at 25 °C, λ_{ex} = 388 nm, λ_{max} = 448 - 474 nm. (b) Fluorescence excitation spectra of T0 (2.6 mM) in 99 % water/THF mixture, λ_{em} = 465 nm. (c) Fluorescence emission spectra of T0 in different water % in water/THF mixture (vol %). (d) Plot of relative intensity (I/I_0) of T0 at 25 °C, λ_{ex} = 388 nm, in different water % in water/THF mixture (vol %).

Formation of inclusion complex with α-CD

Pseudorotaxanes are supramolecular structures that formed between a host (e.g. cyclodextrin, curcubiturils) and guests (e.g. PEG) in aqueous solution due to hydrophobic interaction of the long hydrocarbon chains (guest) with the inner surface of the host.[23, 30, 36, 37] The inclusion complex formed between PEG and α-CD is widely reported due to its relatively

good solubility in water (relative to β-cyclodextrin) and their ability to self-assemble and aggregate in solution.[26-29] α-CD is known to self-assemble in the following ways: i) Formation of the inclusion complex with PEG chains (threading process) mainly driven by hydrophobic interaction;[36, 37] ii) The attractive hydrogen-bond interactions between the adjacent cyclodextrins contribute to the formation of columnar (rodlike) structure.[30, 38] The structure can be viewed as the alignment of cyclodextrins along the polymer chains.[38] The intermolecular aggregation leads to the formation of α-CD threaded nanocylinders (gyration radius ≥ 33nm);[26] iii) The nanocylinders that are connected by naked PEG segments, in a higher length scale, aggregate into larger structure.[39]

We next incorporated α-CD with TPE-PEG_2 solution to obtain an inclusion complex or pseudorotaxane. ^{1}H NMR (500 MHz, $CDCl_3$) of the TPE-PEG_2 solution before and after addition of 4 mM of α-CD were analysed to determine host-guest interaction. The spectra in Figure S5 showed that there was no interaction between the phenyl ring and α-CD (at chemical shift of 6-8 ppm), interaction between PEG and α-CD could not be confirmed. In 2D NOSEY ^{1}H NMR (500 MHz, D_2O) spectrum (Figure 4), we observed clear correlation spots between the characteristic peaks of α-CD and PEG (area in the dotted rectangle), at 25 °C, indicating that the structures are mainly based on threaded α-CD. In the 2D ^{1}H NMR spectrum, proton signal H(a) was attributed to -CH_2- on PEG, while H(1)-(6) were assigned to protons on the glucose unit of CD. TPE-PEG_2 self-assembles into micelles in water at 25 °C, at concentration above CMC. TPE segments aggregated in the core and PEG segments interacting with water molecules at the corona, with some PEG segments threaded with α-CD. The naked PEG segments of the inclusion complex at the corona are also in good solvent conditions. When the concentration of α-CD is increased, α-

CD aggregation may form due to intermolecular association between threaded α-CD, resulting in α-CD rodlike tubes or nano-cylinders.[26, 30, 38]

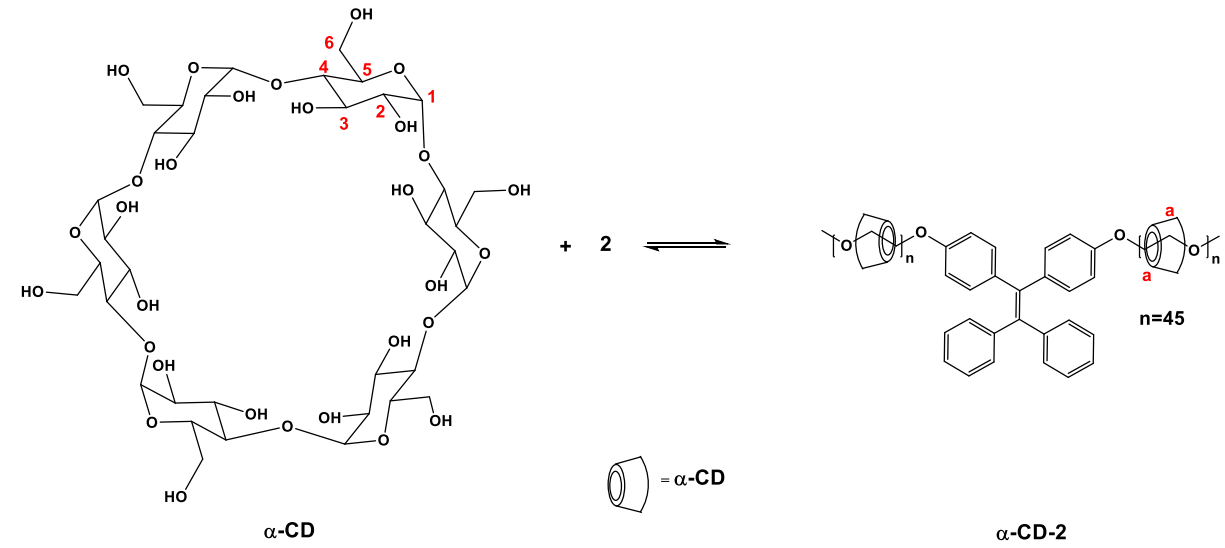

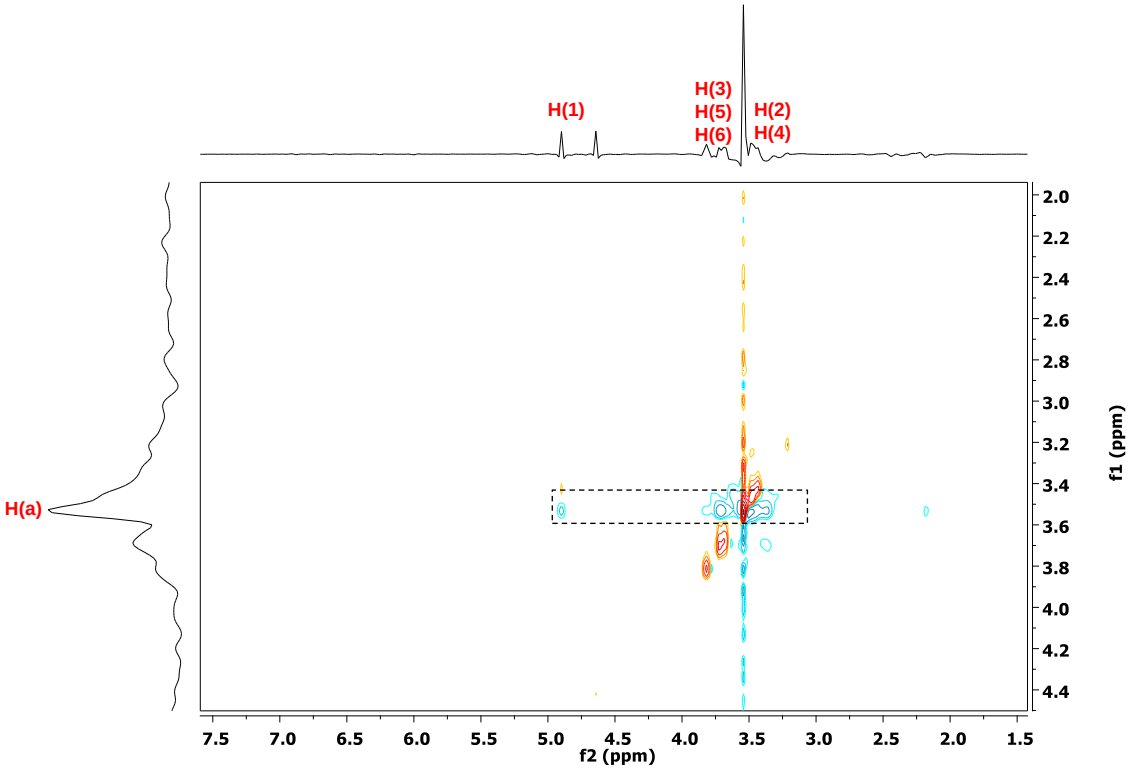

Figure 4. Threading α-cyclodextrin (α-CD) and TPE-PEG_2 (**2**). 2D-NOESY ^{1}H NMR (500 MHz) spectrum of α-CD and TPE-PEG_2 mixture at 25 °C, in D_2O. [α-CD] = 11 mM, [TPE-PEG_2] = 2.6 mM

CMC of TPE-PEG_2 and α-CD mixture at different α-CD concentrations were studied by using DLS analysis. Previous section showed that CMC of TPE-PEG_2 solution was calculated at 23.7×10^{-5} g/mL (6.2×10^{-5} M) (between T5-T6), based on intersection of the two slopes. As shown in Figure 5, after adding 1 mM of α-CD, CMC of the mixture was increased to 46.9×10^{-5} g/mL (1.23×10^{-4} M) (between T4-T5), which could be attributed to greater amount of unimers complexed with cyclodextrin in solution, thus lowering the chance of unimer packing into micelles. Similar results of CMC increase in the mixture of cyclodextrins and sodium dodecyl sulfate (SDS) micelles were reported previously.[40, 41] Further increasing concentration of α-CD (2-4 mM) resulted in increased inhomogeneity in the system. In other words, the addition of CD and the formation of inclusion complex may lead to a mixture of unimers, CD, micelles and dissociated micelles, micelle aggregates and pseudorotaxanes in the solution. Thus, no clear CMC could be calculated based on the graphs obtained (Figure 5(b-d)).

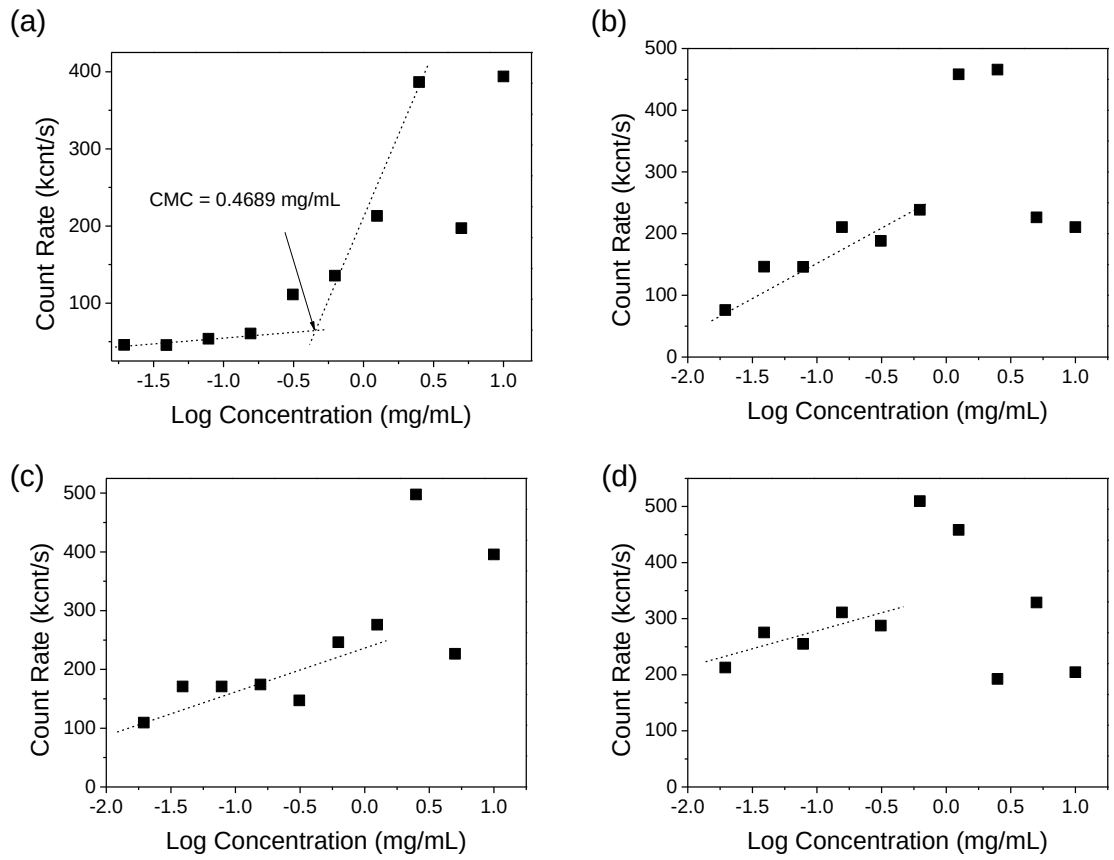

Figure 5. CMC of polymer **2** aqueous solution with addition of various concentrations of α-CD (a) 1 mM, (b) 2 mM, (c) 3 mM and (d) 4 mM, determined by DLS. The intersection of the tangents to the two slopes of the graph where the log concentration was plotted versus count rate at 25 °C.

Figure 6 (a) shows the micelles size decrement after addition of α-CD. When CD is added, the pseudorotaxane structure no longer resembles a normal micelle.[40, 41] The particle size and morphology were examined by atomic force microscopy (AFM), as shown in Figure 6 (b-c). The reduction in particle size after addition of CD was confirmed by AFM, with the change of diameter estimated from around 80 nm (TPE-PEG_2 micelle aggregates, in Figure 6(b)) to pseudorotaxanes diameter of around 35 nm (Figure 6(c)).

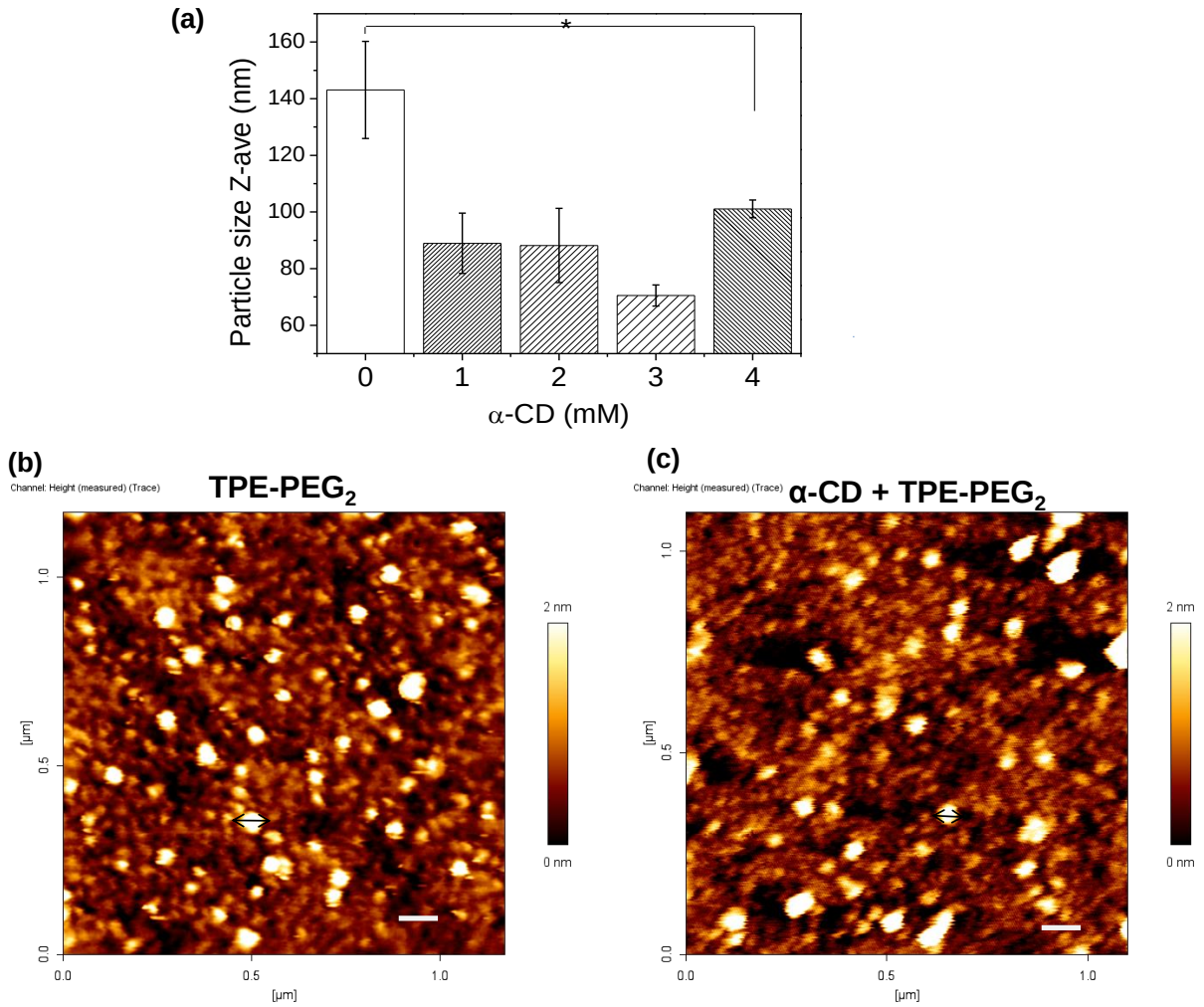

Figure 6. (a) Particle size of [TPE-PEG_2] = 8.2×10^{-2} mM, before and after addition of [α-CD] = 1 - 4 mM, determined by DLS at 25 °C. (at 4 mM, there could be more free CD present) (b) Particle diameter (black arrow) and morphology of TPE-PEG_2 **d ~ 80 nm,** scale bar represents

100 nm. (c) Pseudorotaxane **d ~ 35 nm**, scale bar represents 100 nm, determined by Atomic Force Microscope (AFM) at 25 °C.

The emission efficiency of TPE-PEG_2 pseudorotaxanes was examined by fluorescent assay. Figure 7(a) showed the fluorescent intensity of T0 ([TPE-PEG_2] = 2.6 mM) before and after adding different α-CD concentrations. The change in FL intensity was obvious especially when 2 mM of CD was added. Figure 7(b) highlighted the numerical improvement of FL intensity. The increase in FL emission due to formation of pseudorotaxanes was about 12 times. This is significant when we compare our result with a couple of similar studies. In a TPE-oligo EG solution (n=2-4), a FL emission quenching effect was observed when γ-CD was added due to de-aggregation of hydrophobic TPE segments when being covered in the cavity of γ-CD.[42] In another study, a 2.5 times of FL enhancement was achieved due to micelles precipitation.[34] FL emission intensity of TPE-PEG_2 solution was increased after addition of α-CD, as shown in Figure 7. PEG and α-CD can form host-guest inclusion complex based on threading process, as reported in previous studies.[36, 37] The formation of host-guest inclusion complex between TPE-PEG_2 and α-CD was proven by 2D NOSEY NMR in Figure 4. Therefore, the FL emission enhancement could be attributed to the increase of the number of TPE-PEG_2 chains threaded with α-CD, limiting chain motion both in linear unimers, and in micellar assemblies. The increment of FL emission reached a plateau when 2-4 mM of CD was added. It was attributed to the fact that when there is sufficient CD added and the solution is mainly as inclusion complex, the system is no longer a micellar system.[43] And FL emission was reduced when 5 mM of CD was added (FL emission spectrum not shown) due to de-aggregation and dissociation of micellar structures. A schematic drawing of the formation of CD-threaded unimers and CD-threaded micelles was shown in Figure 8.

β-CD were not used in the investigation of AIE effect, mainly because if it limited solubility in water. This will affect the yield of crystalline pseudorotaxane formation. γ-CD (1 mM) was added to [TPE-PEG_2] = 2.6 mM for comparison of AIE effect, as shown in Figure S7. Our observation is similar with previous study mention above, adding γ-CD resulted in reduction in FL intensity.

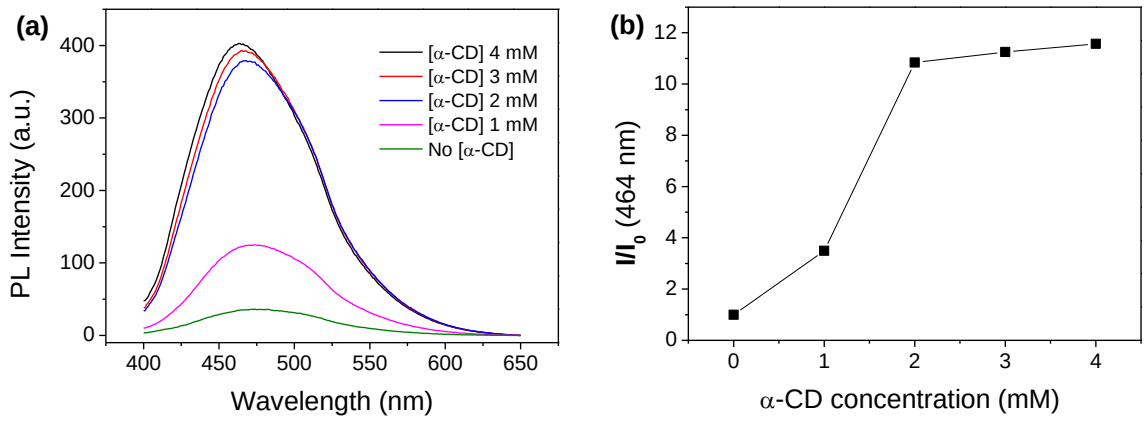

Figure 7. (a) Fluorescence spectra of T0 [TPE-PEG_2] 2.6 mM before and after addition of [α-CD] = 1 - 4 mM, at 25 °C, λ_{ex} = 388 nm, λ_{max} = 464 nm. (b) Comparison of relative fluorescent intensity at 464 nm (blue fluorescent).

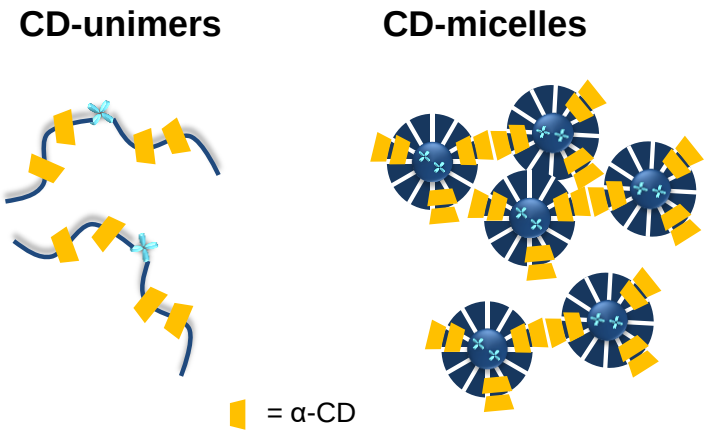

Figure 8. Schematic drawing of pseudorotaxanes solution that consisted of CD-unimers and CD-micelles

Fluorescent intensity of TPE-PEG_2 in cells is elevated by the addition of α-CD

In order to examine the internalization of TPE-PEG_2, A549 cells were treated with 2 mg/ml each of TPE-PEG_2 either alone or in combination with α-CD (stock solutions 40 mg/ml in cell culture medium) for 4 h. Confocal microscopy of cells treated with TPE-PEG_2 showed dull 'blue' fluorescence in the cytoplasm (Figure 9(a)). Addition of equal amount of α-CD to TPE-PEG_2 (final concentration of 2 mg/ml each) significantly enhanced the fluorescence intensity of TPE-PEG_2 and relatively stronger 'blue' fluorescence was detected in the cytoplasm of treated cells in comparison to cells treated with TPE-PEG_2 alone (Figure 9(a),(b)). There was no obvious 'blue' fluorescence in the nucleus suggesting that the TPE-PEG_2 was not internalized into the nucleus and specifically taken up into the cytoplasm.

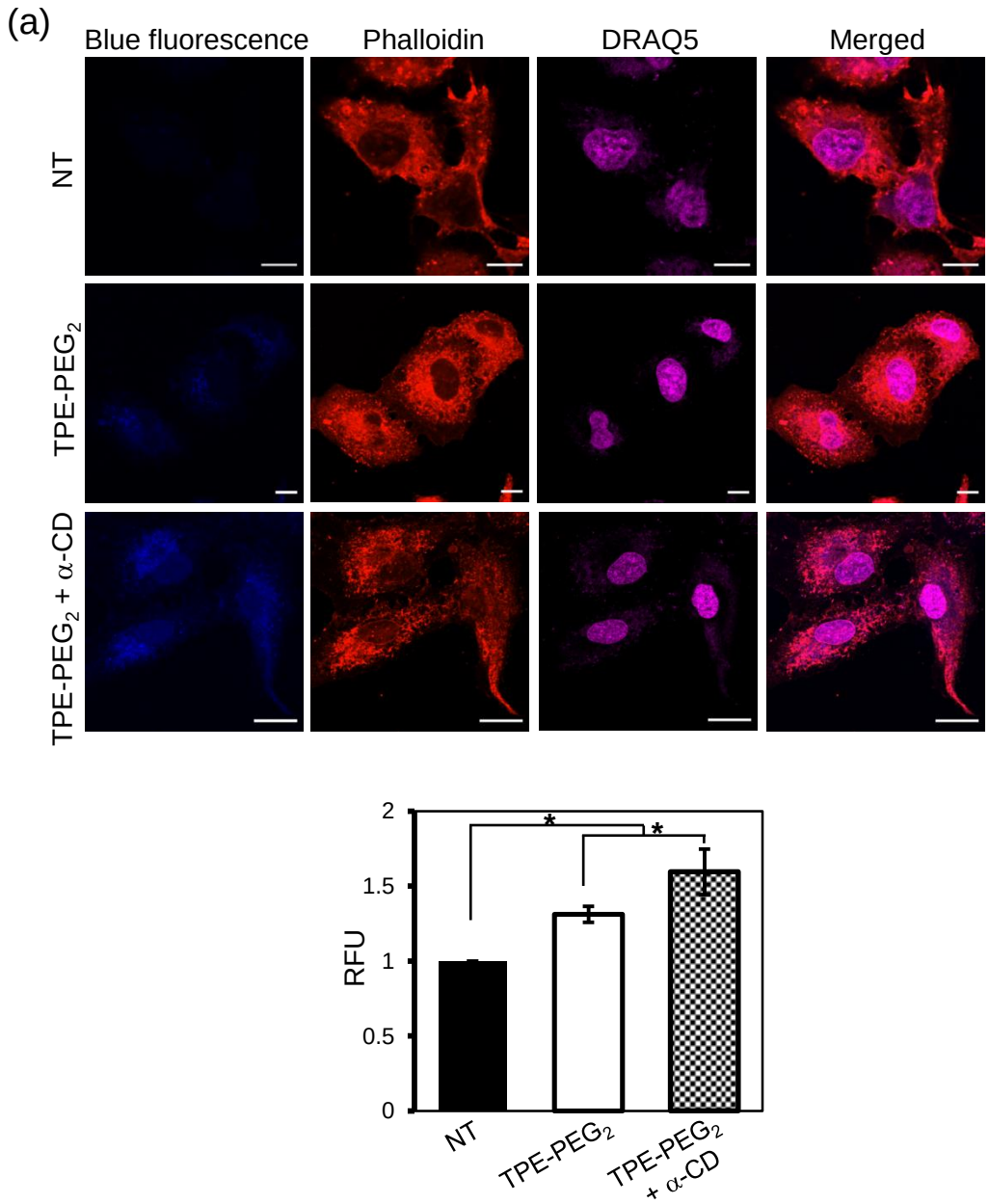

Figure 9. Cellular uptake of TPE-PEG$_2$ by A549 cells. (a) A549 cells seeded on coverslips were treated with 2 mg/ml of TPE-PEG$_2$ or a combination of TPE-PEG$_2$ and α-CD (2 mg/ml each) for 4 h at 37°C and fixed. Untreated cells served as control (NT). Cells were counterstained with rhodamine-phalloidin to visualize cellular morphologies (red) and DRAQ5 to visualize nuclei (purple). Intracellular uptake of TPE-PEG$_2$ (blue florescence) was detected by confocal microcopy and representative images are shown. Scale bar 10 μm. (b) Bar graph shows relative fluorescence unit (RFU) of TPE-PEG$_2$ as analyzed automatically by IN Cell Investigator software. Data represents mean ± SEM of three independent experiments from five random fields per sample per experiment. *$p<0.05$.

TPE-PEG_2 and α-CD are biocompatible to mammalian cells

We examined the cytocompatibility of TPE-PEG_2 and α-CD in three different human cell types - alveolar basal epithelial cell line A549, primary dermal fibroblasts (DF) and liver epithelial cell line HepG2. Cells seeded in 96-well plates were treated with various concentrations of the TPE-PEG_2, α-CD or both (62.5, 125, 250, 500, 1000 and 2000 μg/ml) for 24 h and cellular and nuclear morphologies were quantified using High Content analysis (HCA). Data showed that either TPE-PEG_2, α-CD or a combination of both were biocompatible with little or no cytotoxicity even at the concentration of 2000 μg/ml. Various morphological parameters, including cell 1/form-factor, cell area, cell gyration and nuclear area were within the normal range of variation after treatment with TPE-PEG_2 and α-CD in comparison to that of untreated control cells (NT) (Figure 10 (a), (b)). However, nocodazole, a toxic drug used as a positive control, showed a marked change in gross morphology of cells and nuclei as compared to untreated cells (Figure 10 (a), (b)).

Next, we determined cell viability in the presence of TPE-PEG_2, α-CD or both by MTS-based assay, which is a colorimetric method widely used for quantifying the number of viable cells in a population. The method is based on conversion of MTS to formazan and the quantity of formazan measured by the amount of 490 nm absorbance is directly proportional to the number of living cells in a population. MTS assay showed that there was no major reduction in the viability of A549, DF and HepG2 cells due to the treatment with various concentrations (62.5 – 2000 μg/ml) of TPE-PEG_2, α-CD or a combination of both (Figure 10 (c)). Overall, both HCA

and MTS-based cell viability assays conformed that TPE-PEG_2 and α-CD are biocompatible to mammalian cells.

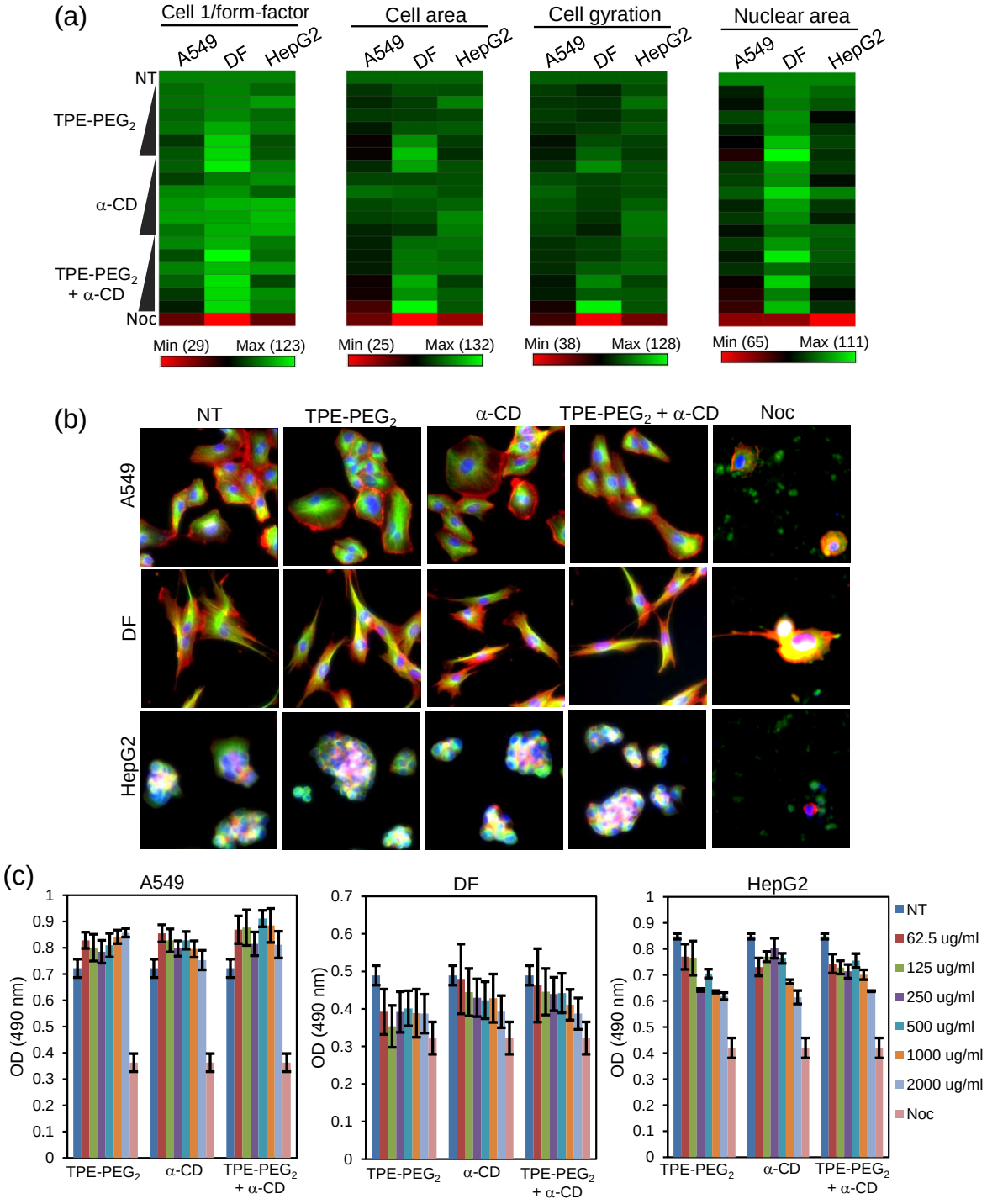

Figure 10. **Multi-parametric biocompatibility analysis of TPE-PEG$_2$.** (**a**) A549, DF and HepG2 cells seeded in 96-well plates were treated with increasing concentrations (62.5, 125, 250, 500, 1000, 2000 μg/ml) of TPE-PEG$_2$, α-CD or both for 24 h. Cells were fixed and stained with rhodamine-phalloidin (red) and Alexa Fluor 488 conjugated anti-α-tubulin (green) to visualize cellular morphologies and Hoechst 33258 (blue) to visualize nuclei. Images were acquired using IN Cell Analyzer 2200 automated microscope. Multiple morphological parameters (cell 1/form-factor, cell area, cell gyration and nuclear area) were automatically quantified by IN Cell Investigator software. Normalized values in terms of percentage change in comparison to that obtained from corresponding untreated control (NT) cells (indicated in parenthesis of the legends below each heat-map tables) were automatically converted into colour gradient-coded heat-maps (spanning from minimum values "red" through the mean "black" to the maximum "green") and presented. (b) Representative images of the cells treated with 500 μg/ml compounds are shown. (c) Bar graphs showing absorbance values [OD (450 nm), mean ± SEM] of A549 (n=9), DF (n=6) and HepG2 (n=3) cells after treatment with TPE-PEG2, α-CD or both for 24 h as determined by MTS assay. Noc, cells treated with nocodazole as toxicity control.

Conclusions

A new strategy for highly efficient AIE by formation of AIE pseudorotaxanes was demonstrated in this study. Amphiphilic TPE-PEG$_2$ exhibited typical AIE behavior in aqueous solution and in solid state. Enhancement in AIE FL intensity was achieved by first, transformation from unimer to micelle state, and second, the formation of pseudorotaxanes with micelles. The AIE-active pseudorotaxane molecule is more superior than most of AIE micelles as the former showed significantly (12 times) higher emission, thanks to the enhanced RIR process in the α-CD cavities. *In vitro* studies showed that the cellular fluorescent emission signals was enhanced with the formation of AIE pseudorotaxanes. The AIE pseudorotaxane polymer was non-toxic, and did not enter the nucleus. These observations suggest that a new biocompatible AIE pseudorotaxane based on host-guest interaction of TPE-PEG$_2$ and α-CD is an excellent FL formulation for cell imaging.

Author Contributions

The manuscript was written through contributions of all authors. All authors have given approval to the final version of the manuscript.

ACKNOWLEDGMENT

N.K.V. acknowledges funding support from Lee Kong Chian School of Medicine, Nanyang Technological University [Start-Up Grant] and the Ministry of Education Singapore [MOE AcRF Tier 1 grant 2014-T1-001-141]. The authors would like to express gratitude to the A*STAR Personal Care Grant (Project no.1325400026) for support of this project.

ABBREVIATIONS

DRAQ5, Deep Red fluorescing AnthraQuinone Nr. 5; SEM, standard error of the mean; CD, cyclodextrin; THF, tetrahydrofuran; DMSO, dimethyl sulfoxide.

Supporting Information

The Supporting Information is available free of charge on the ACS Publications website at

NMR spectra of copolymers with and without cyclodextrins, FTIR spectra of the copolymers, AFM profiles of the inclusion complex aggregates, fluorescence measurements of the polymers in the presence of cyclodeextrin.

REFERENCES

1. Hong, H.; Yang, Y.; Zhang, Y.; Cai, W., Non-Invasive Cell Tracking in Cancer and Cancer Therapy. *Current topics in medicinal chemistry* **2010,** 10, (12), 1237-1248.
2. Keshavan, M., Experimental cancer therapy holds great promise — but at great cost. *STAT news* 23 Aug 2016, 2016.
3. Thoms, S. T-cell therapy news 'holds great promise' in cancer fight. (22 Nov 2016),
4. Wang, Z.; Chen, S.; Lam, J. W.; Qin, W.; Kwok, R. T.; Xie, N.; Hu, Q.; Tang, B. Z., Long-term fluorescent cellular tracing by the aggregates of AIE bioconjugates. *Journal of the American Chemical Society* **2013,** 135, (22), 8238-45.
5. Yu, Y.; Feng, C.; Hong, Y.; Liu, J.; Chen, S.; Ng, K. M.; Luo, K. Q.; Tang, B. Z., Cytophilic fluorescent bioprobes for long-term cell tracking. *Advanced materials* **2011,** 23, (29), 3298-302.
6. Luo, J.; Xie, Z.; Lam, J. W. Y.; Cheng, L.; Chen, H.; Qiu, C.; Kwok, H. S.; Zhan, X.; Liu, Y.; Zhu, D.; Tang, B. Z., Aggregation-induced emission of 1-methyl-1,2,3,4,5-pentaphenylsilole. *Chemical communications* **2001**, (18), 1740-1741.
7. Ding, D.; Li, K.; Liu, B.; Tang, B. Z., Bioprobes based on AIE fluorogens. *Accounts of Chemical Research* **2013,** 46, (11), 2441-2453.
8. Zhang, X.; Wang, K.; Liu, M.; Zhang, X.; Tao, L.; Chen, Y.; Wei, Y., Polymeric AIE-based nanoprobes for biomedical applications: recent advances and perspectives. *Nanoscale* **2015,** 7, (27), 11486-11508.
9. Mei, J.; Leung, N. L. C.; Kwok, R. T. K.; Lam, J. W. Y.; Tang, B. Z., Aggregation-Induced Emission: Together We Shine, United We Soar! *Chemical Reviews* **2015,** 115, (21), 11718-11940.
10. Xu, B.; Zhang, J.; Tian, W., Aggregation-Induced Emission of 9,10-Distyrylanthracene Derivatives and Their Applications. In *Aggregation-Induced Emission: Fundamentals*

Tang, B. Z.; Qin, A., Eds. John Wiley & Sons: 2013.
11. Liow, S. S.; Karim, A. A.; Loh, X. J., Biodegradable thermogelling polymers for biomedical applications. *MRS Bulletin* **2016,** 41, (7), 557-566.
12. Dong, Y.; Lam, J. W. Y.; Li, Z.; Qin, A.; Tong, H.; Dong, Y.; Feng, X.; Tang, B. Z., Vapochromism of Hexaphenylsilole. *Journal of Inorganic and Organometallic Polymers and Materials* **2005,** 15, (2), 287-291.
13. Dong, Y.; Lam, J. W. Y.; Qin, A.; Li, Z.; Sun, J.; Dong, Y.; Tang, B. Z., Vapochromism and Crystallization-Enhanced Emission of 1,1-Disubstituted 2,3,4,5-Tetraphenylsiloles. *Journal of Inorganic and Organometallic Polymers and Materials* **2007,** 17, (4), 673-678.
14. Xue, X.; Zhao, Y.; Dai, L.; Zhang, X.; Hao, X.; Zhang, C.; Huo, S.; Liu, J.; Liu, C.; Kumar, A.; Chen, W. Q.; Zou, G.; Liang, X. J., Spatiotemporal drug release visualized through a drug delivery system with tunable aggregation-induced emission. *Advanced materials* **2014,** 26, (5), 712-7.
15. Zhang, C.; Jin, S.; Li, S.; Xue, X.; Liu, J.; Huang, Y.; Jiang, Y.; Chen, W. Q.; Zou, G.; Liang, X. J., Imaging intracellular anticancer drug delivery by self-assembly micelles with aggregation-induced emission (AIE micelles). *ACS applied materials & interfaces* **2014,** 6, (7), 5212-20.
16. Liow, S. S.; Dou, Q.; Kai, D.; Li, Z.; Sugiarto, S.; Yu, C. Y. Y.; Kwok, R. T. K.; Chen, X.; Wu, Y.-L.; Ong, S. T.; Kizhakeyil, A.; Verma, N. K.; Tang, B. Z.; Loh, X. J., Long-Term Real-Time In Vivo Drug Release Monitoring with AIE Thermogelling Polymer. *Small* **2016**, 1603404-n/a.
17. Wang, H.; Zhao, E.; Lam, J. W. Y.; Tang, B. Z., AIE luminogens: emission brightened by aggregation. *Materials Today* **2015,** 18, (7), 365-377.
18. Tong, H.; Hong, Y.; Dong, Y.; Haussler, M.; Lam, J. W.; Li, Z.; Guo, Z.; Guo, Z.; Tang, B. Z., Fluorescent "light-up" bioprobes based on tetraphenylethylene derivatives with aggregation-induced emission characteristics. *Chemical communications* **2006**, (35), 3705-7.

19. Hong, Y.; Lam, J. W.; Tang, B. Z., Aggregation-induced emission: phenomenon, mechanism and applications. *Chemical communications* **2009**, (29), 4332-53.
20. Liow, S. S.; Dou, Q.; Kai, D.; Li, Z.; Sugiarto, S.; Yu, C. Y. Y.; Kwok, R. T. K.; Chen, X.; Wu, Y.-L.; Ong, S. T.; Kizhakeyil, A.; Verma, N. K.; Tang, B. Z.; Loh, X. J., Long-Term Real-Time In Vivo Drug Release Monitoring with AIE Thermogelling Polymer. *Small* **2016**, (in press).
21. Hong, Y.; Häußler, M.; Lam, J. W. Y.; Li, Z.; Sin, K. K.; Dong, Y.; Tong, H.; Liu, J.; Qin, A.; Renneberg, R.; Tang, B. Z., Label-Free Fluorescent Probing of G-Quadruplex Formation and Real-Time Monitoring of DNA Folding by a Quaternized Tetraphenylethene Salt with Aggregation-Induced Emission Characteristics. *Chemistry – A European Journal* **2008,** 14, (21), 6428-6437.
22. Li, D.; Yu, J.; Xu, R., Mesoporous silica functionalized with an AIE luminogen for drug delivery. *Chemical communications* **2011,** 47, (39), 11077-11079.
23. Li, J.; Loh, X. J., Cyclodextrin-based supramolecular architectures: syntheses, structures, and applications for drug and gene delivery. *Adv Drug Deliv Rev* **2008,** 60, (9), 1000-17.
24. Szejtli, J., *Cyclodextrin Technology*. Kluwer Academic Publishers: The Netherlands, 1988.
25. Bender, M. L.; Komiyama, M., *Cyclodextrin Chemistry*. Springer-Verlag: Berlin, 1978; p Chapters 2 and 3.
26. Travelet, C.; Schlatter, G.; Hebraud, P.; Brochon, C.; Lapp, A.; Hadziioannou, G., Formation and self-organization kinetics of alpha-CD/PEO-based pseudo-polyrotaxanes in water. A specific behavior at 30 degrees C. *Langmuir : the ACS journal of surfaces and colloids* **2009,** 25, (15), 8723-34.
27. Abdul Karim, A.; Loh, X. J., Design of a micellized alpha-cyclodextrin based supramolecular hydrogel system. *Soft Matter* **2015,** 11, (27), 5425-34.
28. Ye, H.; Owh, C.; Loh, X. J., A thixotropic polyglycerol sebacate-based supramolecular hydrogel showing UCST behavior. *RSC Adv.* **2015,** 5, (60), 48720-48728.
29. Kai, D.; Low, Z. W.; Liow, S. S.; Abdul Karim, A.; Ye, H.; Jin, G.; Li, K.; Loh, X. J., Development of lignin supramolecular hydrogels with mechanically responsive and self-healing properties. *ACS Sustainable Chemistry & Engineering* **2015,** 3, (9), 2160-2169.
30. Girardeau, T. E.; Zhao, T.; Leisen, J.; Beckham, H. W.; Bucknall, D. G., Solid Inclusion Complexes of α-Cyclodextrin and Perdeuterated Poly(oxyethylene). *Macromolecules* **2005,** 38, (6), 2261-2270.
31. Ramakrishnam Raju, M. V.; Lin, H.-C., Self-Assembly of Tetraphenylethene-Based [2]Catenane Driven by Acid–Base-Controllable Molecular Switching and Its Enabled Aggregation-Induced Emission. *Organic letters* **2014,** 16, (21), 5564-5567.
32. Tang, L.; Jin, J. K.; Qin, A.; Zhang Yuan, W.; Mao, Y.; Mei, J.; Zhi Sun, J.; Zhong Tang, B., A fluorescent thermometer operating in aggregation-induced emission mechanism: probing thermal transitions of PNIPAM in water. *Chemical communications (Cambridge, England)* **2009**, (33), 4974-4976.
33. Wang, H.; Liu, G.; Gao, H.; Wang, Y., A pH-responsive drug delivery system with an aggregation-induced emission feature for cell imaging and intracellular drug delivery. *Polymer Chemistry* **2015,** 6, (26), 4715-4718.
34. Yin, X.; Meng, F.; Wang, L., Thermosensitivity and luminescent properties of new tetraphenylethylene derivatives bearing peripheral oligo(ethylene glycol) chains. *Journal of Materials Chemistry C* **2013,** 1, (41), 6767.
35. Connell, M. J.; Bachilo, S. M.; Huffman, C. B.; Moore, V. C.; Strano, M. S.; Haroz, E. H.; Rialon, K. L.; Boul, P. J.; Noon, W. H.; Kittrell, C.; Ma, J.; Hauge, R. H.; Weisman, R. B.; Smalley, R. E., Band Gap Fluorescence from Individual Single-Walled Carbon Nanotubes. *Science* **2002,** 297, (5581), 593.
36. Harada, A.; Li, J.; Kamachi, M., Preparation and properties of inclusion complexes of polyethylene glycol with .alpha.-cyclodextrin. *Macromolecules* **1993,** 26, (21), 5698-5703.
37. Li, J.; Harada, A.; Kamachi, M., Sol-Gel Transition during Inclusion Complex Formation between [alpha]-Cyclodextrin and High Molecular Weight Poly(ethylene glycol)s in Aqueous Solution. *Polym J* **1994,** 26, (9), 1019-1026.

38. Topchieva, I. N.; Tonelli, A. E.; Panova, I. G.; Matuchina, E. V.; Kalashnikov, F. A.; Gerasimov, V. I.; Rusa, C. C.; Rusa, M.; Hunt, M. A., Two-Phase Channel Structures Based on α-Cyclodextrin−Polyethylene Glycol Inclusion Complexes. *Langmuir : the ACS journal of surfaces and colloids* **2004,** 20, (21), 9036-9043.
39. Chung, J. W.; Kang, T. J.; Kwak, S.-Y., Supramolecular Self-Assembly of Architecturally Variant α-Cyclodextrin Inclusion Complexes as Building Blocks of Hexagonally Aligned Microfibrils. *Macromolecules* **2007,** 40, (12), 4225-4234.
40. Al-Sherbini, E.-S. A. M., Study the effect of α,β,γ-cyclodextrins on the critical micelles concentration (c.m.c.) of sodium dodecyl sulphate (SDS) by using 1-methyl-4-[4′-aminostyryl]pyridinium iodide. *Colloids and Surfaces A: Physicochemical and Engineering Aspects* **2009,** 352, (1–3), 1-4.
41. Tsianou, M.; Fajalia, A. I., Cyclodextrins and surfactants in aqueous solution above the critical micelle concentration: where are the cyclodextrins located? *Langmuir : the ACS journal of surfaces and colloids* **2014,** 30, (46), 13754-64.
42. Song, S.; Zheng, H. F.; Li, D. M.; Wang, J. H.; Feng, H. T.; Zhu, Z. H.; Chen, Y. C.; Zheng, Y. S., Monomer emission and aggregate emission of TPE derivatives in the presence of gamma-cyclodextrin. *Organic letters* **2014,** 16, (8), 2170-3.
43. Suzaki, Y.; Taira, T.; Takeuchi, D.; Osakada, K., Competing Supramolecular Assembly of Amphiphiles to Form Micelles or Pseudorotaxanes. *Organic Latters* **2007,** 9, (5), 887-890.